NeuroImage 43 (2008) 10–19

Contents lists available at ScienceDirect

NeuroImage

journal homepage: www.elsevier.com/locate/ynimg

Brain white matter damage in SCA1 and SCA2. An in vivo study using voxel-based morphometry, histogram analysis of mean diffusivity and tract-based spatial statistics

Riccardo Della Nave [a], Andrea Ginestroni [a], Carlo Tessa [b], Elena Salvatore [c], Domenico De Grandis [d], Rosaria Plasmati [e], Fabrizio Salvi [e], Giuseppe De Michele [c], Maria Teresa Dotti [f], Silvia Piacentini [g], Mario Mascalchi [a,*]

[a] Radiodiagnostic Section, Department of Clinical Physiopathology, University of Florence, Florence, Viale Morgagni 85, 50134 Florence, Italy
[b] Radiodiology Unit, Versilia Hospital, Camaiore (Lucca), Italy
[c] Department of Neurological Sciences, University of Naples Federico II, Naples, Italy
[d] Department of Neurology, Rovigo Hospital, Rovigo, Italy
[e] Department of Neurology, Bellaria Hospital, University of Bologna, Bologna, Italy
[f] Department of Neurological and Behavioural Sciences, University of Siena, Siena, Italy
[g] Department of Neurological and Psychiatric Sciences, University of Florence, Florence, Italy

ARTICLE INFO

Article history:
Received 1 April 2008
Revised 16 June 2008
Accepted 24 June 2008
Available online 11 July 2008

Keywords:
Voxel-based morphometry
Tract-based spatial statistics-MR imaging
Ataxia
Spinocerebellar ataxia type 1
Spinocerebellar ataxia type 2
Olivopontocerebellar atrophy

ABSTRACT

Background and purpose: Neurodegeneration in spinocerebellar ataxia type 1(SCA1) and 2(SCA2) is associated with white matter(WM) damage. Voxel-Based Morphometry(VBM), histogram analysis of mean diffusivity (MD) and Tract-Based Spatial Statistics(TBSS) enable an in vivo quantitative analysis of WM volume and structure. We assessed with these 3 techniques the whole brain WM damage in SCA1 and SCA2.
Patients and methods: Ten patients with SCA1, 10 patients with SCA2 and 10 controls underwent MRI with acquisition of T1-weighted and diffusion tensor images. The results were correlated with severity of clinical deficit.
Results: VBM showed atrophy of the brainstem and cerebellar WM without significant differences between SCA1 and SCA2. Focal atrophy of the cerebral subcortical WM was also present. Histogram analysis revealed increased MD in the brainstem and cerebellum in patients with SCA1 and SCA2 which in SCA2 was more pronounced and combined with mild increase of the MD in the cerebral hemispheres in SCA2. In SCA1 and SCA2 TBSS revealed decreased fractional anisotropy(FA) in the inferior, middle and superior cerebellar peduncles, pontine transverse fibres, medial and lateral lemnisci, spinothalamic tracts, corticospinal tracts and corpus callosum. The extent of tract changes was greater in SCA2 patients who also showed decreased FA in the short intracerebellar tracts. In both diseases VBM, histogram and TBSS results correlated with clinical severity.
Conclusions: Brain WM damage featuring a pontocerebeellar atrophy is similar in SCA1 and SCA2 but more pronounced in SCA2. In both diseases it correlates with severity of the clinical deficit.

Introduction

Spinocerebellar ataxia type 1(SCA1) and type 2(SCA2) are due to a CAG repeat expansion in two genes coding for proteins of unknown function named ataxin 1 and ataxin 2 and account for 6% and 15%, respectively, of cases of autosomal dominant cerebellar ataxias (Schöls et al., 2004). Neuropathological examination in SCA1 and SCA2 show a macroscopic pattern of olivopontocerebellar atrophy (OPCA) combined with neuronal loss in several brainstem and cerebellar nuclei and cerebellar cortex and a diffuse damage of the brainstem and cerebellar white matter(WM) (Durr et al., 1995; Gilman et al., 1996; Iwabuchi et al., 1999; Estrada et al., 1999; Pang et al., 2002). These features are variably depicted in vivo by MRI (Klockgether et al., 1998; Mascalchi et al., 1998; Giuffrida et al., 1999; Brenneis et al., 2003; Mandelli et al., 2007; Della Nave et al., 2008b; Ginestroni et al., 2008).

Voxel-based morphometry (VBM) is an unbiased whole-brain quantitative method to explore gray matter (GM) and WM atrophy that was applied to the investigation of degenerative ataxias including SCA1 and SCA2 (Brenneis et al., 2003; Della Nave et al., 2008b; Ginestroni et al., 2008). In the last years the capability of diffusion weighted and diffusion tensor MR imaging(DTI) to demonstrate WM damage has found increasing application for the structural evaluation of the normal and abnormal brain (Mori and Zhang, 2006). In

* Corresponding author. Fax: +39 055431970.
E-mail address: m.mascalchi@dfc.unifi.it (M. Mascalchi).

1053-8119/$ – see front matter © 2008 Elsevier Inc. All rights reserved.
doi:10.1016/j.neuroimage.2008.06.036

particular, histogram analysis of the apparent diffusion coefficient (ADC) was successful in demonstrating the diffuse WM abnormality in the brainstem and cerebellum of patients with SCA1 and SCA2 (Guerrini et al., 2004). Recently, a voxel-wise whole-brain analysis of multi-subject diffusion tensor data named Tract-Based Spatial Statistics(TBSS) was developed (Smith et al., 2006, 2007) and preliminarily applied to detect brain WM tract damage in Freidreich ataxia (Della Nave et al., 2008a). We assessed with VBM, histogram analysis of mean diffusivity (MD) computed from DTI and TBSS the brain WM damage in patients with SCA1 and SCA2 and correlated the findings with severity of clinical deficit and disease duration.

Patients and methods

Ten patients (7 women and 3 men; mean age 46±11 years) with genetically proven SCA1 and ten patients (3 women and 7 men; mean age 46±13 years) with genetically proven SCA2 and regularly followed at the ambulatories for ataxias of the Universities of Florence, Naples, Bologna and Siena and of the Rovigo General Hospital in Italy gave their informed consent to participate in this prospective study which was carried out in Florence and approved by the Local Ethical Committee. Molecular diagnostic methods were previously reported (Pareyson et al., 1999) and the cut-off number of triplets repeats expansion qualifying for diagnosis was 40 CAG on one allele for SCA1 and 34 CAG on one allele for SCA2. The mean number of abnormal triplets was 49±10 in SCA1 and 39±1 in SCA2.

The day of the MR examination the same neurologist blind to the results of MR defined the patient's disease duration and computed her or his score on International Cooperative Ataxia Rating Scale (ICARS) (Trouillas et al., 1987). The ICARS is a 0–100 score semiquantitative scale with 100 corresponding to maximal clinical deficit.

The mean disease duration was 10±6 years in SCA1 and 11±9 years in SCA2 and the mean ICARS score 43±28 in SCA1 and 33±19 in SCA2.

Dividing the ICARS scores into thirds of increasing clinical deficit, three SCA1 and four SCA2 patients had a mild deficit (0–33 score), five SCA1 and six SCA2 patients had a moderate deficit (34–67 score) and two SCA1 patients had a severe deficit (68–100 score). Of the 20 patients only one SCA1 carrier was asymptomatic.

Ten age matched healthy volunteers without personal of familial history of neurological disease (4 women and 6 men; mean age 45±11 years) served as controls.

MR examination

Patients and controls underwent MR imaging examination in a single centre on a 1.5 T system (Philips Intera, Best, The Netherlands) with 33 mT/m maximum gradient strength and SENSE coil technology. After scout and axial proton density and T2 weighted images (TR=2242 ms, TE 20/90 ms, FOV=256 mm, matrix size 256×288, 20 slices, slice thickness=5 mm, NEX=2), axial DTI with single-shot echo planar imaging sequence (TR=9394 ms, TE=89 ms, FOV=256 mm, matrix size=128×128, 50 slices, slice thickness=3 mm, no gap, NEX=3) was also acquired on axial plane. Diffusion sensitizing gradients were applied along 15 non-collinear directions using *b value* of 0 (b_0 image) and 1000 s/mm^2. After both automatic segmentation of the brain from the non-brain tissue and correction for simple head motion and distortions due to eddy currents by means of FDT 2.0 (FMRIB's Diffusion Toolbox 2.0) (Behrens et al., 2003) part of FSL 4.0 (FMRIB Software Library, FMRIB Image Analysis Group, Oxford, UK) (Smith et al., 2004) maps of fractional anisotropy (FA), mean diffusivity (MD), and of the greatest (λ_1), middle (λ_2) and smallest (λ_3) individual eigenvalues of the diffusion tensor were calculated from DTI.

To assess regional atrophy, patients and controls were also examined with sagittal 3D T1 weighted turbo gradient echo [repetition time (TR)=8.1 ms, echo time (TE)=3.7 ms, flip angle=8°, inversion time=764 ms, field of view (FOV)=256 mm, matrix size=256×256, 160 contiguous slices, slice thickness=1 mm] images for VBM.

Data processing

Preliminarily proton density and T2 weighted images were subjectively evaluated for signal abnormalities which can influence TBSS results. Moreover DTI derived maps and T1 weighted images were visually evaluated for motion artefacts before entering further image processing.

Image data processing was performed on a PC running the statistical parametric mapping 2 (SPM2) software (Wellcome Department of Cognitive Neurology, London, UK) for VBM and FSL 4.0 package for TBSS.

The methodology of VBM closely followed that previously reported (Good et al., 2001) and included seven steps: reorientation according to the antero-posterior commissure line; template creation to improve brains segmentation; normalization; segmentation in 3 classes of tissue (GM, WM and CSF); modulation; smoothing with a 8 mm full width half-maximum Gaussian kernel; voxelwise statistical analysis.

Histogram analysis was performed on the maps of the MD according to a previously reported procedure (Della Nave et al., 2004; Guerrini et al., 2004). In particular the histogram of the brainstem and cerebellum and of the cerebral hemisphere were calculated and the 25th and 50th (median) percentile and kurtosis of the MD was calculated.

TBSS analysis was performed using TBSS 1.1 tool part of the FSL 4.0 and is described in detail elsewhere (Smith et al., 2006, 2007). In brief, TBSS implies a four step approach: identification of a common registration target and alignment of all subject's FA images to this target; creation of the mean of all aligned FA images and of a skeletonized mean FA image which is thresholded; projection of each subject's FA image onto the skeleton; voxelwise statistic analysis across subject on the skeleton-space FA data. Using the same nonlinear registration, skeleton and skeleton projection vectors derived from the FA, MD, λ_1 and $\lambda_2+\lambda_3/2$ (evaluating parallel and radial diffusion, respectively) data were projected onto the skeleton before voxelwise statistic analysis across subject (Smith et al., 2007).

Statistical methods

VBM

Statistical analysis of the MR data was based on the general linear model and the theory of Gaussian random fields. A voxelwise comparison of spatially normalized T1 weighted images was made using SPM2. Group comparisons were performed by means of analysis of covariance (ANCOVA) using the total volume of each segmented image (GM volume for GM analysis, WM volume for WM analysis) as confounding covariate. Age and gender were included as covariates of no interest to exclude possible effects of these variables on regional GM or WM volumes (Good et al., 2001).

Voxel-level analysis with a significance threshold set at p-value<0.05 corrected for multiple comparisons across the whole brain [false discovery rate (FDR) correction] was applied to the resulting t-statistic maps of GM and WM.

In order to correlate the amount of GM or WM volume loss with clinical features and genetic abnormality, the multiple significant areas of decreased GM or WM at group analyses were saved and applied as a single region of interest (ROI) of fixed volume on normalized modulated GM or WM images of each patient (Della Nave et al., 2008b; Ginestroni et al., 2008). Then the amount of GM, or WM in the ROI was calculated as average value taking into account that in the voxels contained in the ROI the possible value GM or WM is comprised between 0 (null) and 1 (100%). Extracted average volumes for each region of decreased GM or WM were correlated to disease

duration and ICARS score by means of the Spearman rank correlation test.

To achieve a more accurate spatial localization of the significant clusters identified at VBM, we used the Montreal Neurological Institute space utility (Sergey Pakhomov; http://www.ihb.spb.ru/~pet_lab/MSU/MSUMain.html) and the (Schmahmann et al., 1999) atlas for the cerebellum.

Histogram analysis

Differences between SCA1 and SCA2 patients vs controls and each other were assessed with the Mann–Whitney U test. The correlation of the MD histogram metrics of the brainstem and cerebellum with the clinical score and disease duration was assessed using the Spearman rank correlation test.

TBSS

Group comparison for FA, MD, λ_1 and $\lambda_2+\lambda_3/2$ data was performed using permutation-based nonparametric inference on cluster size (Nichols and Holmes, 2002) and Randomise 2.0 software part of FSL 4.0. A restrictive statistical thresholds was used (cluster-based thresholding $t>3$, $p<0.05$, corrected for multiple comparisons) (Smith et al., 2006).

In addition, in SCA1 and SCA2 patients we correlated FA and MD with each patient's ICARS score and disease duration using the same software and permutation-based nonparametric inference on cluster size ($t>3$, $p<0.05$ corrected) (Smith et al., 2006).

Identification of the abnormal WM tracts revealed by TBSS was based on the Atlas made at Johns Hopkins University (Wakana et al., 2004, Mori et al., 2005, Wakana et al., 2007) and the Kretschmann and Weinrich textbook of Cranial Neuroimaging and Clinical Neuroanatomy (2004).

Results

Proton density and T2 weighted images showed the “cruciform” or “hot bun” sign characteristic of OPCA in the basis pontis of 6 SCA1 and 5 SCA2 patients. Multiple small focal hyperintensities were observed in one patient with SCA1, two patients with SCA2 and in no controls.

Table 1
SCA1: VBM results for volumes of gray and white matter in 10 SCA1 patients

	Cluster size (mm^3)	Voxel		MNI Coordinates (local maxima)			Areas
		T	P_{FDR}	x	y	z	
GM: Controls >SCA1	63701	8.01	0.002	−9	−38	−30	R cerebellar hemisphere (lobules III, IV, V, VI, Crus I, Crus II, VIIb, VIII, IX), L cerebellar hemisphere (lobules III, IV, V, VI, VIII, IX), cerebellar vermis (lobules III, IV, V, VI)
	1072	6.72	0.002	34	−23	64	R precentral and postcentral gyri
	179	5.79	0.002	45	−39	3	R middle and superior temporal gyri
	183	4.74	0.006	−46	12	16	L inferior frontal operculum gyrus
	1290	4.69	0.006	40	−35	51	R inferior parietal, R postcentral, R suprmarginal gyri
	170	4.00	0.016	−42	−68	21	L middle temporal and middle occipital gyri
	576	3.79	0.022	10	−72	−44	R cerebellar hemisphere (lobules Crus II, VIIb, VIII)
WM: Controls >SCA1	6907	6.27	0.034	−8	−35	−44	Peridentate regions, middle cerebellar peduncles, dorsal portion of the brainstem

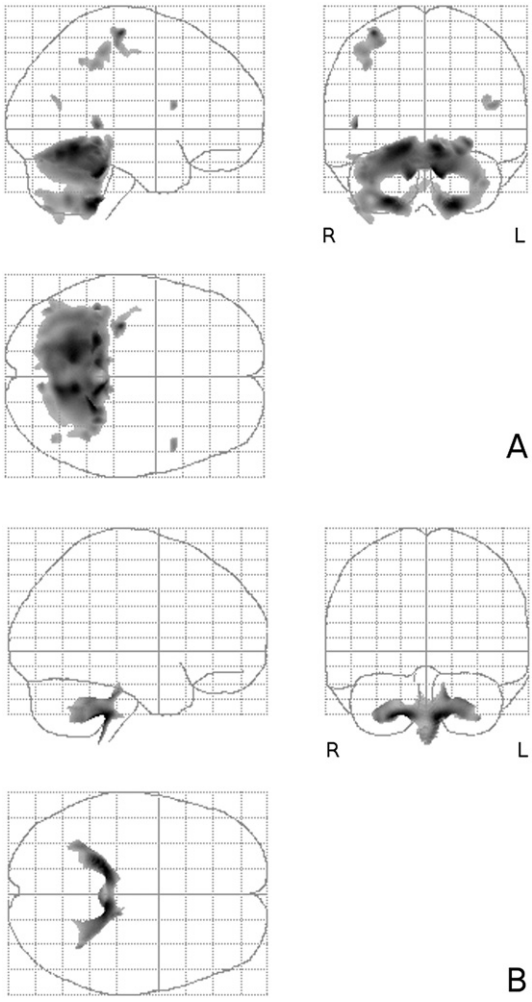

Fig. 1. (A, B) VBM analysis. Maps of the t-value (voxel analysis at $p<0.05$ FDR corrected for multiple comparisons) represented as glass brain showing the patterns of GM (A) and WM (B) loss in SCA1 patients as compared to healthy controls. Panel A shows symmetric extensive loss of cortical GM in the cerebellar hemispheres and vermis as well as multiple small clusters of GM loss in the cerebral hemispheres (listed in Table 1). Panel B demonstrated symmetric WM loss in the peridentate regions and middle cerebellar peduncles combined with atrophy of the dorsal portion of the brainstem. No cluster of reduced WM volume is observed in the cerebral hemispheres.

Enlargement of the CFS spaces was present in 4 patients with SCA1 and 4 patients with SCA2. No motion artefacts in DTI derived maps and T1 weighted images were visually appreciated in patients and controls.

SCA1

VBM

Symmetric extensive loss of cortical GM was observed in the cerebellar hemispheres and vermis with sparing of lobules I, II, and X (Table 1 and Fig. 1). Small clusters of GM loss were also observed in multiple cerebral regions bilaterallty (see Table 1).

Symmetric WM loss was observed in the peridentate regions and middle cerebellar peduncles combined with atrophy of the dorsal portion of the brainstem (Table 1 and Fig. 1). No cluster of reduced WM volume was seen in the cerebral hemispheres.

A correlation was observed between ICARS score and decreased brainstem and cerebellar WM volume ($R=-0.67$; $p=0.03$), whereas the correlation with GM cerebellar volume loss was not significant ($R=-0.54$; $p=0.10$). No correlation of GM or WM loss with disease duration was observed.

Table 2
Results of mean diffusivity ($\times 10^{-3}$ mm^2/s) histograms in SCA1, SCA2 and Healthy controls

		SCA1	SCA2	Controls
Brainstem and cerebellum	25th percentile	0.76±0.05**	0.85±0.10***,a	0.67±0.01
	50th percentile	0.89±0.09**	1.09±0.24***,a	0.74±0.02
	Kurtosis	5.4±1.8**	5.2±2.4*	8.8±2.2
Cerebral hemispheres	25th percentile	0.71±0.03	0.72±0.01*	0.70±0.00
	50th percentile	0.80±0.05	0.80±0.02**	0.78±0.00
	Kurtosis	8.1±2.7	9.3±2.2	10.5±3.0

* $p<0.05$ of the difference between SCA1 or SCA2 patient group and control group.
** $p<0.01$ of the difference between SCA1 or SCA2 patient group and control group.
*** $p<0.001$ of the difference between SCA1 or SCA2 patient group and control group.
[a] $p<0.05$ of the difference between SCA1 and SCA2 patient group.

Histogram analysis

The 25th and 50th percentile of the MD histogram of the brainstem and cerebellum were significantly higher and the kurtosis was significantly lower in SCA1 patients than in controls (Table 2). The MD histogram of the cerebral hemisphere was not significantly different in SCA1 patients and controls (Table 2).

The correlation of the 25th ($R=0.56$; $p=0.08$) or 50th ($R=0.55$; $p=0.09$) percentile of brainstem and cerebellar MD with ICARS score was not significant while that of the same 50th percentile with disease duration was borderline ($R=0.61$; $p=0.05$). Kurtosis of the brainstem and cerebellar MD histogram did not correlate with ICARS score ($R=-0.13$;$p=0.70$) whereas its correlation with disease duration was not significant ($R=-0.59$; $p=0.07$).

TBSS

Decreased FA were present in the inferior cerebellar peduncle, superior cerebellar peduncle, medial and lateral lemnisci and spinothalamic tract, bilaterally. Clusters of decreased FA were also observed in the transverse pontine fibres, right middle cerebellar peduncle, corpus callosum and the left corticospinal tract at the level of the corona radiata and the right corticopinal tract in the pons (Table 3 and Fig. 2). Areas of significantly increased MD were generally more extensive and were localized in the brainstem and cerebellar WM (Fig. 3). They only partially overlapped with areas of decreased FA. Their distribution was similar to that of the areas of significantly increased $\lambda_2+\lambda_3/2$, whereas the analysis of λ_1 maps revealed that while most of the tracts identified because of their decreased FA showed increased λ_1 the medial and lateral lemnisci and the spinothalamic tracts in the dorsal pons demonstrated a significantly decreased λ_1. No areas of significantly decreased $\lambda_2+\lambda_3/2$ were observed. ICARS score correlated with decreased FA in the inferior and superior cerebellar peduncles and with increased MD in multiple areas of the brainstem, cerebellum and cerebral hemispheres (Suppl. Fig. 1). No correlation of decreased FA or increased MD with disease duration was observed.

SCA2

VBM

Extensive loss of cortical cerebellar GM volume was observed in the entire cerebellum with sparing of the cerebellar lobules I, II and X (Table 4 and Fig. 4). Additional clusters of decreased GM volume were observed in the right thalamus and in the cerebral hemispheres including left precentral and inferior frontal operculum gyrus and inferior parietal and post-central gyrus.

Reduced WM was observed symmetrically in the peridentate regions, middle cerebellar peduncles, dorsal portion of the brainstem and ventral portion of the pons (Table 4 and Fig. 4). Two additional cluster of reduced WM volume were present in the left precentral gyrus and right middle cingulum gyrus.

An inverse correlation was observed between the brainstem and cerebellar GM ($R=-0.92$; $p<0.001$) and WM volume ($R=-0.78$; $p=0.006$) and ICARS score but not between the same volumes and disease duration.

Histogram analysis

The 25th and 50th percentile of the MD histogram of the brainstem and cerebellum were significantly higher and the kurtosis was significantly lower in SCA2 patients than in controls (Table 2). Also the 25th and 50th percentiles of the MD histogram of the cerebral hemisphere was significantly higher in SCA2 patients than in controls (Table 2).

The correlation of the 25th ($R=0.79$; $p<0.01$), 50th ($R=0.71$; $p<0.05$) percentile or kurtosis ($R=-0.74$; $p<0.01$) of brainstem and cerebellar MD with ICARS score was significant as well as the correlation of the same kurtosis ($R=-0.67$; $p<0.05$) with disease duration, whereas the correlation of the same 50th percentile with disease duration was not significant ($R=0.59$; $p=0.06$). Borderline correlation ($R=0.62$; $p=0.05$) was also observed between ICARS and the 50th percentile of the MD histogram of the cerebral hemispheres.

TBSS

Decreased FA was observed in the inferior, middle and superior cerebellar peduncles, the deep cerebellar white matter, medial and lateral lemnisci and spinothalamic tract bilaterally and in the transverse pontine fibres (Table 5 and Fig. 5). In addition a nearly symmetric decrease of FA was observed in the corticospinal tracts from the level of the internal capsule, to the bulbar pyramis (Table 5 and Fig. 5). Finally decreased FA was seen in the in the corpus callosum and right inferior longitudinal fasciculus and inferior fronto-occipital fasciculus. Areas of significantly increased MD were generally more extensive and were localized in the brainstem and cerebellar WM (Fig. 6). They only partially overlapped with areas of decreased FA. Their distribution was similar to that of the areas of significantly increased $\lambda_2+\lambda_3/2$ whereas the analysis of λ_1 maps (Fig. 7) revealed that while most of the tracts identified because of their decreased FA showed increased λ_1 the medial and lateral lemnisci and the spinothalamic tracts in the dorsal pons demonstrated a significantly decreased λ_1. No areas of significantly decreased $\lambda_2+\lambda_3/2$ were observed.

No correlation was observed between decreased FA in the WM tracts and ICARS score or disease duration. Increased MD in the WM correlated with ICARS score in a small areas of the left cerebellar hemisphere and in left fornix (Suppl. Fig. 2) while there was no correlation with disease duration.

Table 3
SCA1 TBSS results: decreased FA in SCA1 patients vs Healthy controls

	Cluster size (mm^3)	P	Coordinates (local maxima)			Areas
			x	y	z	
FA: SCA1<Controls	1074	0.001	8	−43	−46	R inferior and superior cerebellar peduncles, R medial and lateral lemnisci, R spinothalamic tract, transverse pontine fibres
	473	0.005	−8	−43	−42	L inferior and superior cerebellar peduncles
	212	0.016	2	−18	24	Body of the corpus callosum
	164	0.025	−4	−34	−37	L medial and lateral lemnisci, L spinothalamic tract
	151	0.031	−18	−25	35	L superior corona radiata (L corticospinal tract)
	141	0.037	5	18	17	Body of the corpus callosum

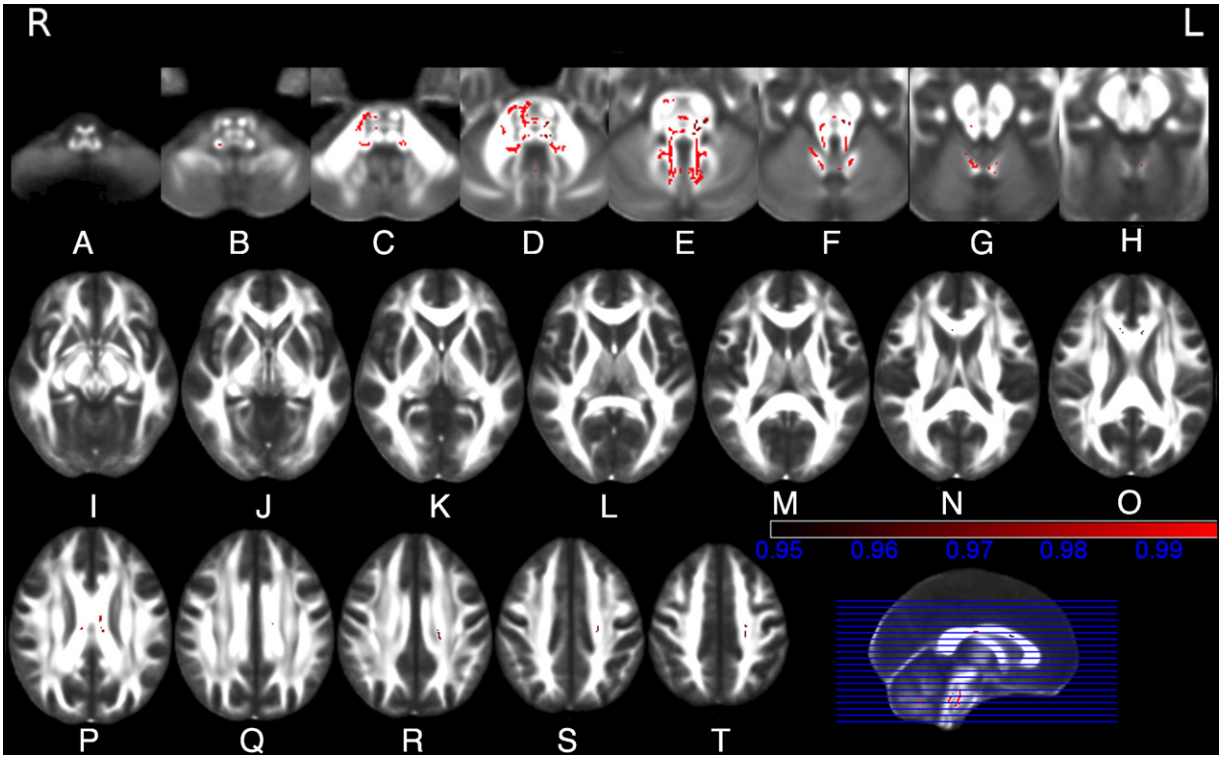

Fig. 2. (A–T). TBSS analysis of FA maps in SCA1 patients vs healthy controls. Maps of the *t*-value ($t>3$ with $p<0.05$ corrected for multiple comparisons) showing in red the clusters of significantly reduced FA in WM tracts in SCA1 patients as compared to controls. These include the inferior cerebellar peduncle (B, C), superior cerebellar peduncle (E, F) and the medial and lateral lemnisci and the spinothalamic tract (D, E, F) bilaterally, the transverse pontine fibres (D,E), the right middle cerebellar peduncle (D), corpus callosum (N, O, P) and the left corticospinal tract at the level of the corona radiata (R, S, T) and the right corticopinal tract in the basis pontis (C, D, E).

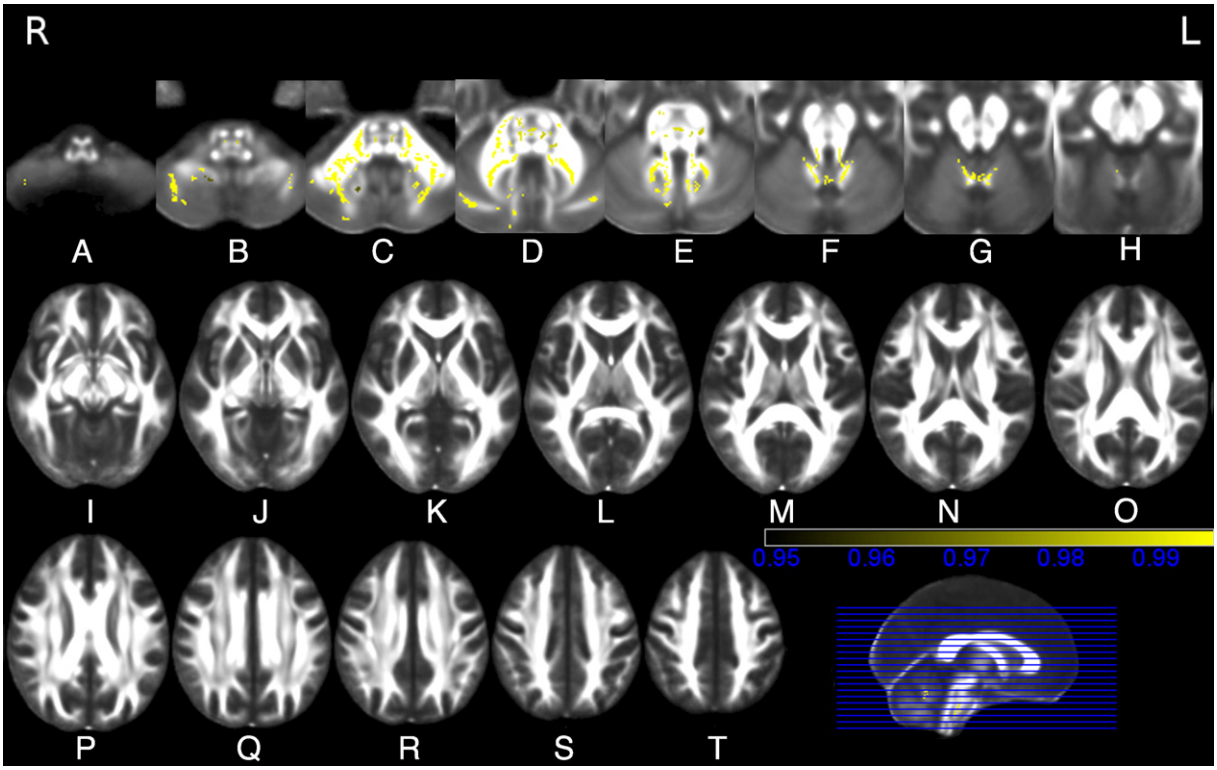

Fig. 3. (A–T). TBSS analysis of MD maps in SCA1 patients vs healthy controls. Maps of the *t*-value ($t>3$ with $p<0.05$ corrected for multiple comparisons) showing in yellow the clusters of significantly increased MD in WM in SCA1 patients as compared to controls. The areas in the brainstem, cerebellar peduncles and cerebellum are generally more extensive but only partially overlapping with those of significantly decreased FA.

Table 4
SCA2 VBM results for volumes of gray and white matter in 10 SCA2 patients

	Cluster size (mm^3)	Voxel		MNI Coordinates (local maxima)			Areas
		T	P_{FDR}	*x*	*y*	*z*	
GM: Controls>SCA2	82935	10.11	0.000	8	−39	−28	R cerebellar hemisphere (lobules III, IV, V, VI, Crus I, Crus II, VIII, IX), L cerebellar hemisphere (lobules IV, V, VI, Crus I, VIII, IX), cerebellar vermis (lobules III, IV, V, VI, VII, VIII)
	265	4.75	0.003	−21	−90	−29	L cerebellar hemisphere (Crus I, Crus II)
	312	4.66	0.004	−50	9	29	L precentral and inferior frontal operculum gyri
	126	4.03	0.011	−39	−38	42	L inferior parietal and postcentral gyri
	1044	3.99	0.012	16	−7	10	R thalamus
WM: Controls>SCA2	16100	8.69	0.001	15	−35	−35	Peridentate regions, middle cerebellar peduncles, dorsal portion of the brainstem and ventral portion of the pons
	431	4.88	0.004	−38	−3	22	L subcortical white matter (precentral gyrus)
	112	3.83	0.031	17	−30	31	R subcortical white matter (middle cingulum gyrus)

SCA1 vs SCA2

VBM

No significant difference for GM, WM or CSF volume was observed between SCA1 and SCA2 patients.

Histogram analysis

The 25th and 50th percentile of the brainstem and cerebellar MD histogram was significantly higher in SCA2 than in SCA1 patients (Table 2). No other MD histogram metrics were significantly different.

TBSS

No significant difference was observed for FA and MD between SCA1 and SCA2 patient groups.

Discussion

Neuropathological examination in SCA1 and SCA2 (Durr et al., 1995; Gilman et al., 1996; Iwabuchi et al., 1999; Estrada et al., 1999; Pang et al., 2002) reveals a pattern of OPCA. However Oppenheimer (1984) noted that degeneration of the inferior olives was secondary to cortical cerebellar lesions and proposed to name the pattern simply as pontocerebellar atrophy. Interestingly, normal bulk of the inferior olives was reported in the largest neuropathological series of SCA2 (Estrada et al., 1999) and no MRI study so far (Klockgether et al., 1998; Mascalchi et al., 1998; Giuffrida et al., 1999), including the present one and three others using VBM (Brenneis et al., 2003; Della Nave et al., 2008b; Ginestroni et al., in press), documented atrophy of the inferior olives in SCA1 or SCA2. This justifies adoption of the term pontocerebellar atrophy to describe the essential macroscopic feature of SCA1 and SCA2.

The microscopic examination shows some heterogeneity in cases of SCA1 and, especially, SCA2. This notwithstanding some differences in the GM involvement between SCA1 and SCA2 were outlined (Iwabuchi et al., 1999; Schöls et al., 2004). In fact, the dentate nucleus is affected in SCA1 and spared in SCA2, whereas the cerebellar cortex and pontine nuclei are more severely damaged in SCA2 than in SCA1. The cerebral hemispheres are essentially spared in SCA1 (Iwabuchi et al., 1999; Gilman et al., 1996), whereas neuronal loss in the thalamus, basal ganglia and cerebral cortex is reported in SCA2 (Durr et al., 1995, Estrada et al., 1999; Pang et al. 2002).

The WM damage in SCA1 or SCA2 received variable attention but was consistently reported by the neuropathologists. Gilman et al. (1996) reported in SCA1 pallor of the WM in myelin stain in the cerebellum and axonal loss and gliosis in the pons. Durr et al. (1995) reported loss of myelinated fibres with gliosis in inferior and middle cerebellar peduncles, cerebellum and fasciculus cuneatus in SCA2. Estrada et al. (1999) reported in SCA2 reduction of the myelinated fibres in the folia as in the central cerebellar WM. Pang et al. (2002) reported that neuronal loss in the brain of SCA2 was accompanied by proportional degree of gliosis.

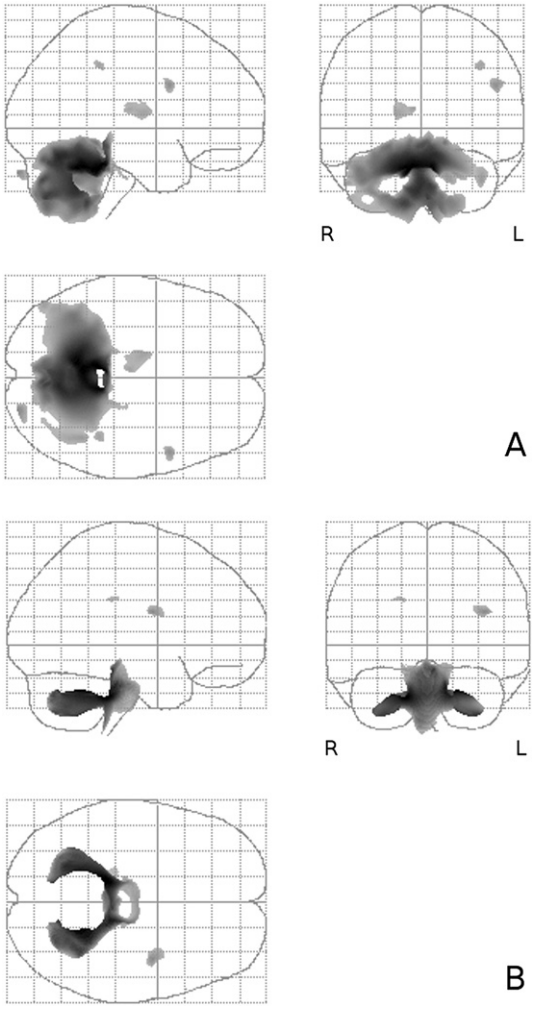

Fig. 4. (A, B). VBM analysis. Maps of the *t*-value (voxel analysis at $p<0.05$ FDR corrected for multiple comparisons) represented as glass brain showing the patterns of GM (A) and WM (B) loss in SCA2 patients as compared to healthy controls. Panel A shows extensive loss of cortical cerebellar GM volume. Additional clusters of decreased GM volume are observed in the right thalamus and in the cerebral hemispheres (listed in Table 3). Panel B demonstrated symmetrically reduced WM in the peridentate regions, middle cerebellar peduncles, dorsal portion of the brainstem and ventral portion of the pons. Two additional cluster of reduced WM volume are present in the left precentral gyrus and right middle cingulum gyrus.

Table 5
SCA2 TBSS results: decreased FA in SCA2 patients vs Healthy controls

	Cluster size (mm^3)	P	Coordinates (local maxima)			Areas
			x	y	z	
FA: SCA2 <Controls	5398	0.000	−2	−41	−60	R and L inferior, middle and superior cerebellar peduncles, R and L medial and lateral lemnisci and spinothalamic tracts, transverse pontine fibres, R and L corticospinal tracts (bulbar pyramids, pons)
	618	0.003	−12	−25	−20	L corticospinal tract (cerebral peduncle and internal capsule)
	548	0.003	11	−18	−20	R corticospinal tract (cerebral peduncle and internal capsule)
	302	0.009	40	−55	−38	R deep cerebellar white matter
	203	0.022	−6	−55	−51	L deep cerebellar white matter
	193	0.024	4	2	24	Body of the corpus callosum
	152	0.037	9	−53	−51	R deep cerebellar white matter
	132	0.045	40	−40	−10	R inferior longitidinal fasciculus and inferior fronto-occipital fasciculus
	129	0.048	−3	18	17	Body of the corpus callosum

Some differential involvement of WM tracts in SCA1 and SCA2 was emphasized (Iwabuchi et al., 1999; Schöls et al., 2004) including prominent damage of spinocerebellar and vestibulocerebellar systems and superior cerebellar peduncles in SCA1 and more pronounced damage of the transverse pontine fibres, middle cerebellar peduncles and intracerebellar WM tracts in SCA2. The involvement of the brain corticospinal tract in SCA1 and SCA2 is controversial. In fact it was reported in 2 out of 8 SCA1 cases (Greenfield, 1954), but was not mentioned by Iwabuchi et al. (1999) who, on the other hand, mentioned atrophy of the cerebral peduncles in SCA2 that was not observed by other Authors (Durr et al., 1995; Estrada et al., 1999). Finally a systematic neuropathological investigation of the central somatosensory system in one patient with SCA2 (Rub et al., 2005) revealed neuronal loss in many relay station of the system, including the Clarke's column of the spinal cord, cuneate, external cuneate and gracile nuclei, trigeminal nuclei and thalamus, and atrophy and demyelination of the interconnecting fiber tracts including posterior spinocerebellar tract, cuneate and gracile fascicles, medial lemniscus and trigeminal tract.

In a MRI study Savoiardo et al. (1990) firstly drew attention to a significant WM damage in OPCA. In fact they reported a diffuse mild signal change of the brainstem and cerebellum in proton density and T2 weighted MR images of 23 patients with sporadic or inherited OPCA. This was accompanied by characteristic sparing of the superior cerebellar peduncles and the pontine cortico-spinal tract, the latter featuring a “cruciform” or “hot cross bun “ sign. The sign was reported in variable percentages in series of patients with SCA1 and SCA2 (Mascalchi et al., 1998; Giuffrida et al., 1999; Mandelli et al., 2007).

In the present study we performed a multi-faceted quantitative evaluation of the whole brain WM in SCA1 and SCA2 using VBM, histogram analysis of MD and TBSS. In particular while VBM demonstrated the pattern of loss of bulk of the WM, histogram analysis enabled evaluation of the diffuse damage of the remaining brainstem, cerebellar and cerebral WM and TBSS identified the structural damage of the main brain WM tracts. The pattern of pontocerebellar WM volume loss VBM demonstrated in our SCA1 and SCA2 patients is in line with prior reports (Klockgether et al., 1998; Mascalchi et al., 1998; Giuffrida et al., 1999; Brenneis et al., 2003). However at variance with two previous VBM studies from our group which included larger number of patients with SCA1 (Ginestroni et al., 2008) or SCA2 (Della Nave et al., 2008b) in the present series we

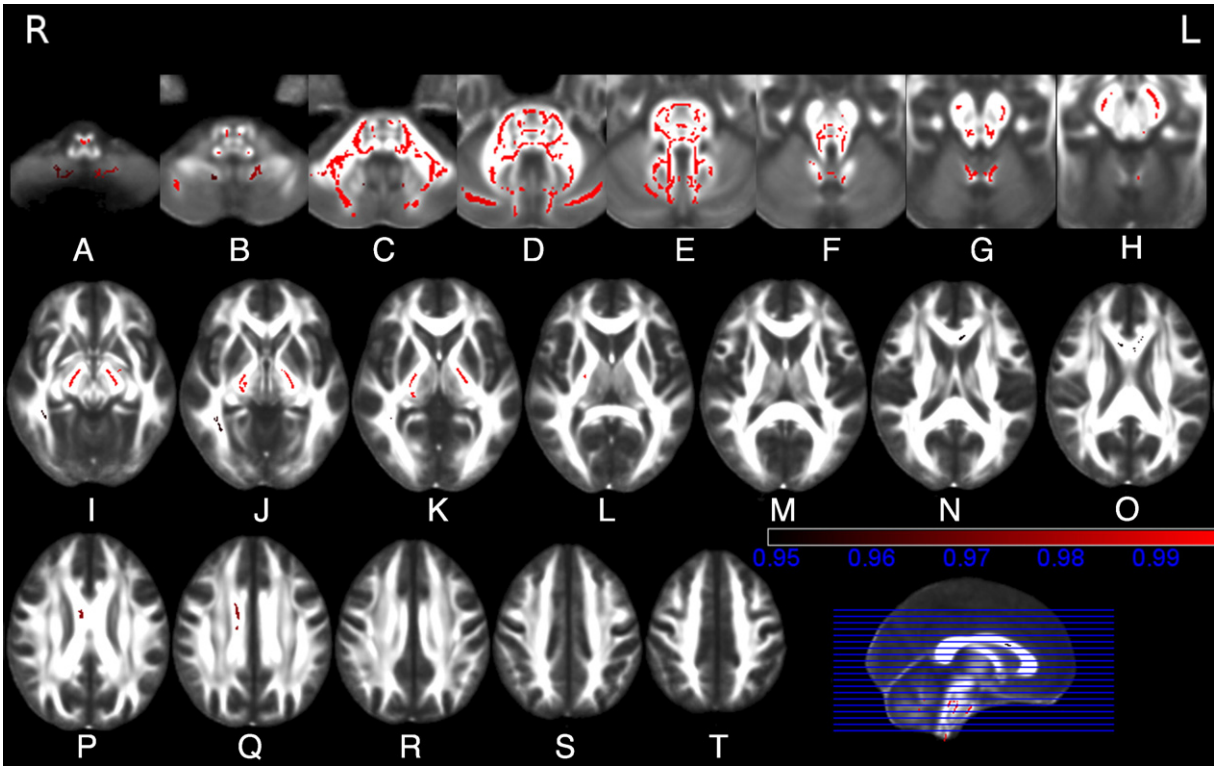

Fig. 5. (A–T). TBSS analysis of FA maps in SCA2 patients vs healthy controls. Maps of the *t*-value ($t>3$ with $p<0.05$ corrected for multiple comparisons) showing in red the clusters of significantly reduced FA in WM tracts in SCA2 patients as compared to controls. These include the inferior (B, C), middle (C, D) and superior (E, F) cerebellar peduncles, the deep cerebellar white matter (C, D, E, F), the medial and lateral lemnisci and the spinothalamic tracts (D, E, F), the transverse pontine fibres (D, E), the corticospinal tracts at the level of the internal capsule (J, K, L), cerebral peduncels (G, H, I), basis pontis (C, D) and bulbar pyramis (A, B), the corpus callosum (N, O, P, Q) and the right inferior longitudinal fasciculus (I, J) and inferior fronto-occipital fasciculus (I, J).

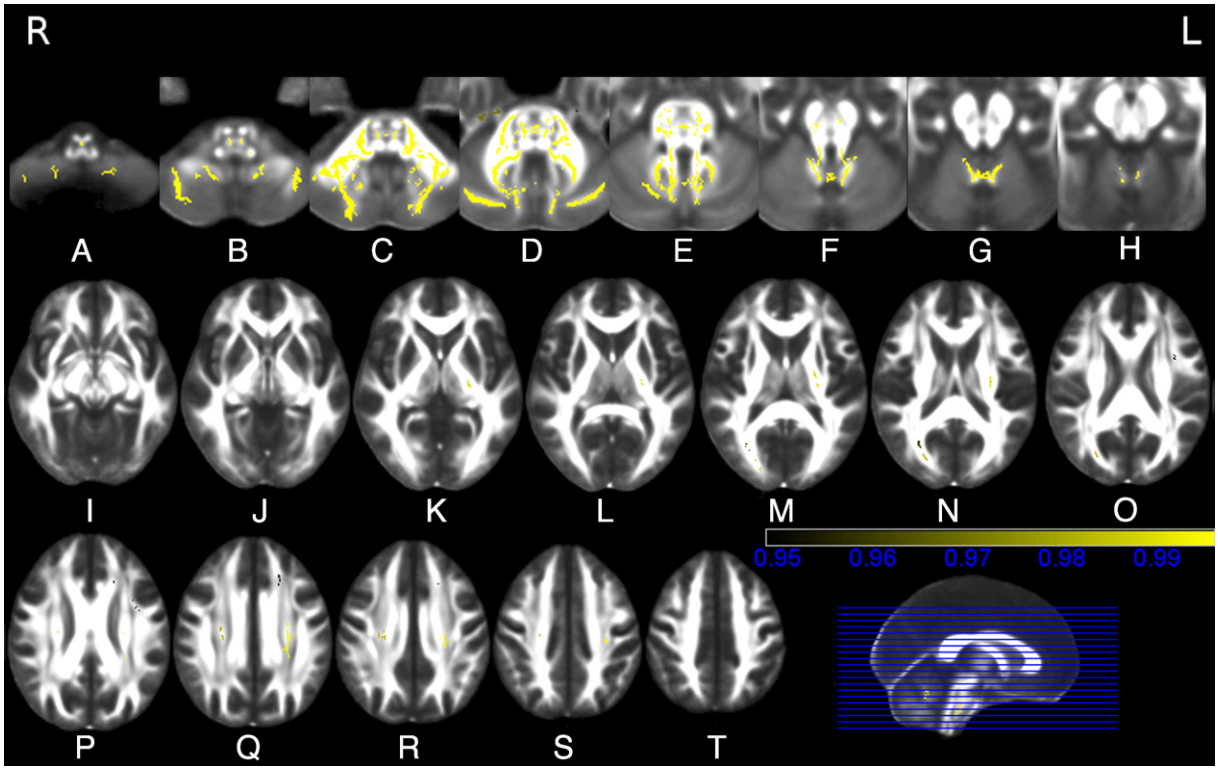

Fig. 6. (A–T). TBSS analysis of MD maps in SCA2 patients vs healthy controls. Maps of the *t*-value ($t>3$ with $p<0.05$ corrected for multiple comparisons) showing in yellow the clusters of significantly increased MD in WM tracts in SCA2 patients as compared to controls. The areas in the brainstem, cerebellar peduncles and cerebellum are generally more extensive but only partially overlapping with those of significantly decreased FA.

observed more extensive atrophy of the middle cerebellar peduncles and of the dorsal brainstem in SCA1, and atrophy of the ventral pons and of two small areas of the cerebral WM in SCA2.

These differences presumably reflect the use in the present investigation of a different more heavily T1-weighted sequence providing a higher contrast between GM, WM and CSF as compared to our previous studies.

Using evaluation of the ADC of water protons with region of interest and histogram analysis we previously reported (Guerrini et al., 2004) an increase of ADC in the brainstem and cerebellum in SCA1 and SCA2. Similar results were obtained by Mandelli et al. (2007) who evaluated with DTI two groups of SCA1 and SCA2 patients and a control group using regions of interest (ROI) centered in the cerebellar WM and several brainstem and cerebellar WM tracts. The results of the present study confirm the value of histogram of MD to detect the diffuse damage of the brainstem and cerebellum in SCA1 and SCA2. It is noteworthy that the only significant difference we found in directly comparing SCA1 and SCA2 patients was the more marked increase of the 25th and 50th percentiles of the brainstem and cerebellar histogram MD suggesting a more severe neurodegeneration of the infratentorial WM in SCA2 in patients. This results is in line with the data of Mandelli et al. (2007). A more severe damage of the brain WM in SCA2 is also supported by the VBM results showing two small areas of WM loss in the cerebral hemisphere as well as by the mild but significant increase of the MD of the cerebral hemispheres that we found in comparing SCA2 patients and controls. The evidence of cerebral WM damage in SCA2 is in line with the neuropathological findings (Durr et al., 1995; Iwabuchi et al., 1999; Estrada et al., 1999; Pang et al., 2002) and the clinical observation of cognitive decline in advanced cases of SCA2 (Schöls et al., 2004).

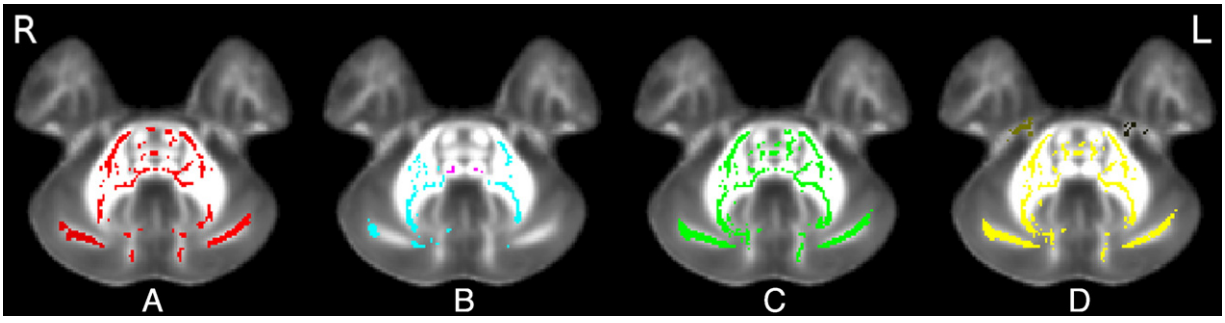

Fig. 7. (A–D). TBSS analysis of the FA (A), λ_1 (B), $\lambda_2+\lambda_3/2$ (C) and MD maps in SCA2 patients vs healthy controls at the level of the middle cerebellar peduncles. Areas of significantly decreased FA (A) are shown in red and include the left corticospinal tract, the transverse pontine fibres, the medial and lateral lemnisci and the spinothalamic tracts, the middle cerebellar peduncels and short intracerebellar fibres. Areas of significantly decreased λ_1 (in pink) include the medial and lateral lemnisci and the spinothalamic tracts (B), while decreased λ_1 (in sky-blue) is observed in the middle cerebellar peduncles and short intracerebellar fibres in the right cerebellar hemisphere. Areas of significantly increased $\lambda_2+\lambda_3/2$ (C) are shown in green and include the left corticospinal tracts, the transverse pontine fibres, the medial and lateral lemnisci and the spinothalamic tracts, the middle cerebellar peduncels and short intracerebellar fibres. Areas of significantly increased MD are shown in yellow (D) and include the transverse pontine fibres, the middle cerebellar peduncles and short intracerebellar fibres.

Using ROI Mandelli et al. (2007) found significantly decreased FA in superior and middle cerebellar peduncles, transverse pontine fibres and midbrain and pontine corticospinal tracts in both SCA1 and SCA2. TBSS has several intrinsic advantages as compared to ROI evaluation. In fact it is less operator-dependent, enables a whole-brain exploration and does not suffer from a prior knowledge bias. In our study TBSS analysis revealed decreased FA in multiple WM tracts of the brainstem, cerebellum and cerebral hemispheres in patients with SCA1 and SCA2 as compared to healthy controls. Albeit with a generally greater extension in SCA2, most WM tracts were affected in both SCA1 and SCA2, including the inferior, middle and superior cerebellar peduncles, transverse pontine fibres, medial and lateral lemnisci, spinothalamic tracts, corticospinal tracts and corpus callosum. In SCA2 only decreased FA was also observed in the intracerebellar WM tracts and the right inferior longitudinal fasciculus and inferior fronto-occipital fasciculus.The majority of these affected tracts match those expected from the neuropathological studies.

The analysis of MD maps in SCA1 and SCA2 as compared to controls showed a more diffuse WM damage which only partially overlapped with the distribution of the WM tracts with decreased FA.

More interesting in our opinion was the demonstration in either group of patients as compared to controls that in some somatosensory WM tracts in the dorsal brainstem (medial and lateral lemnisci and spinothalamic tracts) showing decreased FA this was accompanied by a significant decrease of λ_1 featuring a pattern consistent with wallerian degeneration (Beaulieau et al., 1996; Pierpaoli et al., 2001; Cosottini et al., 2005), while in the remainder of the tracts showing decreased FA there was a significant increase of λ_1 (and $\lambda_2+\lambda_3/2$) featuring a pattern expected in direct WM damage as that observed in stroke and multiple sclerosis (Bammer et al., 2000; Pierpaoli et al., 2001) or a more advanced stage of wallerian degeneration. This finding indicates the capability of DTI analysis supplemented by TBBS in revealing some heterogeneity of the WM tract damage in neurodegenerative diseases as SCA1 and SCA2. This capability deserves further investigation in different neurodegenerative diseases and in greater sample sizes.

Since no significant difference in GM or WM volume loss, selective tract involvement or diffuse WM structural damage as revealed by MD maps was observed when a direct comparison of SCA1 and SCA2 patients was carried out, the only significant difference being a higher value of the MD in the brainstem and cerebellar histogram in SCA2, our overall results support the view that, despite differences in molecular pathology and some clinical features (Schöls et al., 2004), SCA1 and SCA2 share the ultimate pattern of pontocerebellar atrophy (Della Nave et al., 2004; Mandelli et al., 2007).

Overall the present results confirm that a substantial and heterogenous WM damage is part of the neurodegenerative process of pontocerebellar atrophy in general (Savoiardo et al., 1990) and specifically in SCA1 and SCA2 (Mascalchi et al., 1998; Mandelli et al., 2007) and suggest a possible contribute of WM structural damage to clinical disability. However definition of the relationship between GM and WM changes in SCA1 and SCA2 remains to be established. In particular, although inclusions bodies were observed in the nuclei of neurons but also in the cytoplasm of glial cells in SCA1 and SCA2 (Gilman et al., 1996; Pang et al., 2002), changes of the glia have not been fully investigated in SCAs (Schöls et al., 2004). Hence the possibility that WM damage in SCA1 and SCA2 could reflect ongoing damage of the glial cells rather than simply represent wallerian degeneration or dying-back phenomena secondary to GM pathology, should not be discarded. Prospective MRI studies in asymptomatic gene carrier could help to resolve this important issue.

With the advent of molecular genetics tests the diagnostic role of MRI in inherited ataxias has considerably been reduced. However MRI still enables phenotype characterization (see above) and, especially, correlation of clinical variables with measurements of structural damage. In the present investigation each of the 3 methods utilized to measure structural WM damage showed a variable correlation with severity of the clinical deficit and disease duration. The correlation of brainstem and cerebellar WM loss or increased MD with clinical severity in SCA1 or SCA2 confirm and extend prior observations (Brenneis et al., 2003; Guerrini et al., 2004; Mandelli et al., 2007; Della Nave et al., 2008b; Ginestroni et al., 2008). More importantly the correlation in SCA1 of the clinical severity scores with decreased FA in the inferior and superior cerebellar peduncles, containing, respectively, the posterior spinocerebellar tracts and the cerebellofugal fibres arising from the dentate nuclei which are known to show prominent degeneration in SCA1, extends to pontocerebellar degeneration observations previously made using TBSS in amyotrophic lateral sclerosis (Smith et al., 2007) and Freidreich's ataxia (Della Nave et al., 2008a) about the correlation between tract structural damage revealed by DTI and clinical deficit. In our opinion, the fact that no such a correlation was observed in SCA2 and that only kurtosis of the brainstem and cerebellar MD histogram was inversely correlated with disease duration in SCA2 presumably reflect the small number of patients examined. We did not correlate VBM, MD histograms and TBSS findings with the number of triplets but such a correlation was not observed in several prior MRI studies (Schöls et al., 1997; Klockgether et al., 1998; Giuffrida et al., 1999; Brenneis et al., 2003; Della Nave et al., 2008b; Ginestroni et al., 2008).

We recognize some limitations of our study.

The number of patients we examined was small. Hence our results have to be considered as preliminary.

We used DT images with relatively low spatial resolution and labelling of some abnormal WM tracts was difficult, especially in the brainstem in which the anatomic organization of the many WM tracts is much complex. It is expected that DTI at higher magnetic field strength than 1.5 T enabling higher spatial resolution in the same acquisition time will improve delineation and labelling of normal and abnormal brainstem and cerebellar tracts.

We performed a cross-sectional study. Although VBM, histogram analysis of MD and TBSS are well suited for longitudinal evaluation this was not performed in the present investigation. This notwithstanding, the overall correlation between quantitative measurements of pontocerebellar WM damage and severity of clinical impairment seems to justify consideration of these tools as potential outcome measurements besides clinical and paraclinical tests in future therapeutical trials driven by the advances in the molecular pathology of these conditions (Di Prospero and Fishbeck, 2005).

In conclusion, VBM, histogram analysis of MD and TBSS are complementary for an in vivo quantitative assessment of the WM damage featuring a pontocerebellar atrophy pattern that correlates with the severity of the clinical deficit in SCA1 and SCA2. Structural damage of the brainstem, cerebellar and cerebral WM is more pronounced in SCA2. Further longitudinal investigations of the relationship between GM and WM structural abnormalities in asymptomatic carriers of the disease genes are warranted.

Acknowledgments

This study was supported in part by research grants of the National Organization for Rare Disorders Inc. (Danbury, CT, USA) to Professor Mario Mascalchi and of the Italian Ministry of Research and University to Prof. Giuseppe de Michele (PRIN 2005) and to Professor Mario Mascalchi (PRIN 2007).

Appendix A. Supplementary data

Supplementary data associated with this article can be found, in the online version, at doi:10.1016/j.neuroimage.2008.06.036.

References

Bammer, R., Augustin, M., Strasser-Fuchs, S., Seifert, T., Kapeller, Stollberger, R., Ebner, F., Hartung, H.P., Fazekas, F., 2000. Magnetic resonance diffusion tensor imaging for characterizing diffuse and focal abnormalities in multiple sclerosis. Magn. Reson. Med. 44, 583–591.

Beaulieau, C., Does, M.D., Snyder, C., 1996. Changes in water diffusion due to wallerian degeneration in peripheral nerve. Magn. Reson. Med. 36, 627–631.

Behrens, T.E., Woolrich, M.W., Jenkinson, M., Johansen-Berg, H., Nunes, R.G., Clare, S., Matthews, P.M., Brady, J.M., Smith, S.M., 2003. Characterization and propagation of uncertainty in diffusion-weighted MR imaging. Magn. Reson. Med. 50, 1077–1088.

Brenneis, C., Boesch, S.M., Schocke, M., Wenning, G.K., Poewe, W., 2003. Atrophy pattern in SCA2 determined by voxel-based morphometry. Neuroreport. 14, 1799–1802.

Cosottini, M., Giannelli, M., Siciliano, G., Lazzaretti, G., Nichelassi, M.C., Del Corona, A., Bartolozzi, C., Murri, L., 2005. Diffusion-tensor MR imaging of corticospinal tract in amyotrophic lateral sclerosis and progressive muscular atrophy. Radiology. 237, 258–264.

Della Nave, R., Foresti, S., Tessa, C., Moretti, M., Ginestroni, A., Gavazzi, C., Guerrini, L., Salvi, F., Piacentini, S., Mascalchi, M., 2004. ADC mapping of neurodegeneration in the brainstem and cerebellum in patients with progressive ataxias. NeuroImage. 22, 698–705.

Della Nave, R., Ginestroni, A., Tessa, C., Salvatore, E., Bartolomei, I., Salvi, F., Dotti, M.T., De Michele, G., Piacentini, S., Mascalchi, M., 2008a. Brain white matter tracts degeneration in Friedreich ataxia. An in vivo MRI study using Tract-Based Spatial Statistics and Voxel Based Morphometry. NeuroImage. 1, 19–25.

Della Nave, R., Ginestroni, A., Tessa, C., Cosottini, M., Giannelli, M., Salvatore, E., Sartucci, F., De Michele, G., Dotti, M.T., Piacentini, S., Mascalchi, M., 2008b. Brain structural damage in spinocerebellar ataxia type 2. A Voxel-Based Morphometry study. Mov. Disord. 23, 900–904.

Di Prospero, N.A., Fishbeck, K.H., 2005. Therapeutics development for triple repeat expansion disease. Nat. Rev. Genet. 6, 756–765.

Durr, A., Smadja, D., Cancel, G., Lezin, A., Stevanin, G., Mikol, J., Bellance, R., Buisson, G., Chneiweiss, H., Dellanavc, J., Agid, Y., Brice, A., Vernant, J.C., 1995. Autosomal dominant cerebellar ataxia type I in Martinique (French West Indies). Clinical and neuropathological analysis of 53 patients from three unrelated SCA2 families. Brain. 118, 1573–1681.

Estrada, R., Galarraga, J., Orozco, G., Nodarse, A., Auburger, G., 1999. Spinocerebellar ataxia 2 (SCA2): morphometric analysis in 11 autopsies. Acta Neuropathol. 97, 306–310.

Gilman, S., Sima, A.A., Junck, L., Kluin, K.J., Koeppe, R.A., Lohman, M.E., Little, R., 1996. Spinocerebellar ataxia type1 with multiple system degeneration and glial cytoplasmic inclusions. Ann. Neurol. 39, 241–255.

Ginestroni, A., Della Nave, R., Tessa, C., Giannelli, M., De Grandis, D., Piacentini, S., Plasmati, R., Salvi, F., Mascalchi, M., in press. Brain structural damage in spinocerebellar ataxia type 1. A VBM study. J. Neurol. 2008 June 13 [Epub ahead of print].

Giuffrida, S., Saponara, R., Restivo, D.A., Trovato Salinaro, A., Tomarchio, L., Pugliares, P., Fabbri, G., Maccagnano, C., 1999. Supratentorial atrophy in spinocerebellar ataxia type 2: MRI study of 20 patients. J. Neurol. 246, 383–388.

Good, C.D., Johnsrude, I.S., Ashburner, J., Henson, R.N., Friston, K.J., Frackowiak, R.S., 2001. A voxel-based morphometric study of ageing in 465 normal adult human brains. NeuroImage. 14, 21–36.

Greenfield, J.G., 1954. The spinocerebellar degenerations. Blackwell, Oxford.

Guerrini, L., Lolli, F., Ginestroni, A., Belli, G., Della Nave, R., Tessa, C., Foresti, S., Cosottini, M., Piacentini, S., Salvi, F., Plasmati, R., De Grandis, D., Siciliano, G., Filla, A., Mascalchi, M., 2004. Brainstem neurodegeneration correlates with clinical dysfunction in SCA1 but not in SCA2. A volumetric, diffusion and quantitative proton spectroscopy MR study. Brain. 127, 1785–1795.

Klockgether, T., Skalej, M., Wedekind, D., Luft, A.R., Welte, D., Schulz, J.B., Abele, M., Bürk, K., Laccone, F., Brice, A., Dichgans, J., 1998. Autosomal dominant cerebellar ataxia type I. MRI-based volumetry of posterior fossa structures and basal ganglia in spinocerebellar ataxia types 1, 2 and 3. Brain. 121, 1678–1693.

Kretschmann, H., Weinrich, W., 2004. Cranial Neuroimaging and Clinical Neuroanatomy. Atlas of MR Imaging and Computed Tomography, 3rd Edition. Georg Thieme Verlag, Germany.

Iwabuchi, K., Tsuchiya, K., Uchihara, T., Yagishita, S., 1999. Autosomal dominant spinocerebellar degenerations. Clinical, pathological, and genetic correlations. Rev. Neurol. (Paris) 155, 255–270.

Mandelli, M.L., De Simone, T., Minati, L., Bruzzone, M.G., Mariotti, C., Fancellu, R., Savoiardo, M., Grisoli, M., 2007. Diffusion tensor imaging of spinocerebellar ataxias types 1 and 2. AJNR Am. J. Nuroradiol. 28, 1996–2000.

Mascalchi, M., Tosetti, M., Plasmati, R., Bianchi, M.C., Tessa, C., Salvi, F., Frontali, M., Valzania, F., Bartolozzi, C., Tassinari, C.A., 1998. Proton magnetic resonance spectroscopy in an italian family with spinocerebellar ataxia type 1. Ann. Neurol. 43, 244–252.

Mori, S., Wakana, S., van Zijl, P.C.M., Nagae-Poetscher, L.M., 2005. MRI Atlas of Human White Matter. Elsevier, Amsterdam, The Netherland.

Mori, S., Zhang, J., 2006. Principles of diffusion tensor imaging and its applications to basic neuroscience research. Neuron. 51, 527–539.

Nichols, T.E., Holmes, A.P., 2002. Nonparametric permutation tests for functional neuroimaging: a primer with examples. Hum. Brain. Mapp. 15, 1–25.

Oppenheimer, D.R., 1984. Diseases of the basal ganglia and motor neurons. In: Hume, J., Adams, Corsellis, J.A.N., Duchen, L.W. (Eds.), Greenfield's Neuropathology, 4th ed. Wiley, New York, pp. 699–747.

Pang, J.T., Giunti, P., Chamberlain, S., An, S.F., Vitaliani, R., Scaravilli, T., Martinian, L., Wood, N.W., Scaravilli, F., Ansorge, O., 2002. Neuronal intranuclear inclusions in SCA2: a genetic, morphological and immunohistochemical study of two cases. Brain. 125, 656–663.

Pareyson, D., Gellera, C., Castellotti, B., Antonelli, A., Riggio, M.C., Mazzucchelli, F., Girotti, F., Pietrini, V., Mariotti, C., Di Donato, S., 1999. Clinical and molecular studies in 73 Italian families with autosomal dominant cerebellar ataxia type I: SCA 1 and SCA 2 are the most common genotypes. J. Neurol. 246, 389–393.

Pierpaoli, C., Barnett, A., Pajevic, S., Chen, R., Penix, Virta, A., Basser, P., 2001. Water diffusion changes in Wallerian degeneration and their dependance on white matter architecture. NeuroImage. 13, 1174–1185.

Rub, U., Del Turco, D., Burk, K., Diaz, G.O., Auburger, G., Mittelbronn, M., Gierga, K., Ghebremedhin, E., Schultz, C., Schols, L., Bohl, J., Braak, H., Deller, T., 2005. Extended pathoanatomical studies point to a consistent affection of the thalamus in spinocerebellar ataxia type 2. Neuropathol. Appl. Neurobiol. 31, 127–140.

Savoiardo, M., Strada, L., Girotti, F., Zimmerman, R.A., Grisoli, M., Testa, D., Petrillo, R., 1990. Olivopontocerebellar atrophy: MR diagnosis and relationship to multi-system atrophy. Radiology. 174, 693–696.

Schmahmann, J.D., Doyon, J., McDonald, D., Holmes, C., Lavoie, K., Hurwitz, A.S., Kabani, N., Toga, A., Evans, A., Petrides, M., 1999. Three-dimensional MRI atlas of the human cerebellum in proportional stereotaxic space. NeuroImage. 10, 233–260.

Schöls, L., Amoiridis, G., Büttner, T., Przuntek, H., Epplen, J.T., Riess, O., 1997. Autosomal dominant cerebellar ataxia: phenotypic differences in genetically defined subtypes? Ann. Neurol. 42, 924–932.

Schöls, L., Bauer, P., Schmidt, T., Schulte, T., Riess, O., 2004. Autosomal dominant cerebellar ataxias. Lancet Neurol. 3, 291–304.

Smith, S.M., Jenkinson, M., Woolrich, M.W., Beckmann, C.F., Behrens, T.E., Johansen-Berg, H., Bannister, P.R., De Luca, M., Drobnjak, I., Flitney, D.E., Niazy, R.K., Saunders, J., Vickers, J., Zhang, Y., De Stefano, N., Brady, J.M., Matthews, P.M., 2004. Advances in functional and structural MR image analysis and implementation as FSL. NeuroImage. 23, 208–219.

Smith, S.M., Jenkinson, M., Johansen-Berg, H., Rueckert, D., Nichols, T.E., Mackay, C.E., Watkins, K.E., Ciccarelli, O., Cader, M.Z., Matthews, P.M., Beherens, T.E.J., 2006. Tract-based spatial statistics: voxelwise analysis of multi-subject diffusion data. NeuroImage. 31, 1487–1505.

Smith, S.M., Johansen-Berg, H., Jenkinson, M., Rueckert, D., Nichols, T.E., Miller, K.L., Robson, M.D., Jones, D.K., Klein, J.C., Bartsch, A.J., Behrens, T.E., 2007. Acquisition and voxelwise analysis of multi-subject diffusion data with Tract-Based Spatial Statistics. Nature Protocols. 3, 499–503.

Trouillas, P., Takayanagi, T., Hallett, M., Currier, R.D., Subramony, S.H., Wessel, K., Bryer, A., Diener, H.C., Massaquoi, S., Gomez, C.M., Coutinho, P., Ben Hamida, M., Campanella, G., Filla, A., Schut, L., Timann, D., Honnorat, J., Nighoghossian, N., Manyam, B., 1997. International Cooperative Ataxia Rating Scale for pharmacological assessment of the cerebellar syndrome. The Ataxia Neuropharmacology Committee of the World Federation of Neurology. J. Neurol. Sci. 145, 205–211.

Wakana, S., Jiang, H., Nagae-Poetscher, L.M., van Zijl, P.C., Mori, S., 2004. Fiber tract-based atlas of human white matter anatomy. Radiology. 230, 77–87.

Wakana, S., Caprihan, A., Panzenboeck, M.M., Fallon, J.H., Perry, M., Gollub, R.L., Hua, K., Zhang, J., Jiang, H., Dubey, P., Blitz, A., van Zijl, P., Mori, S., 2007. Reproducibility of quantitative tractography methods applied to cerebral white matter. NeuroImage. 36, 630–644.